



## **Thermal conductivity versus depth profiling of inhomogeneous materials using the hot disc technique**

Downloaded from: <https://research.chalmers.se>, 2025-12-06 04:12 UTC

Citation for the original published paper (version of record):

Sizov, A., Cederkrantz, D., Salmi, L. et al (2016). Thermal conductivity versus depth profiling of inhomogeneous materials using the hot disc technique. Review of Scientific Instruments, 87(7): 074901-. <http://dx.doi.org/10.1063/1.4954972>

N.B. When citing this work, cite the original published paper.

RESEARCH ARTICLE | JULY 01 2016

## Thermal conductivity versus depth profiling of inhomogeneous materials using the hot disc technique

A. Sizov ; D. Cederkrantz; L. Salmi ; A. Rosén; L. Jacobson; S. E. Gustafsson; M. Gustavsson



*Rev. Sci. Instrum.* 87, 074901 (2016)

<https://doi.org/10.1063/1.4954972>



Export  
Citation

CrossMark

### Articles You May Be Interested In

Thermal conductivity vs depth profiling using the hot disk technique—Analysis of anisotropic, inhomogeneous structures

*Rev. Sci. Instrum.* (July 2023)

Pulse transient hot strip technique adapted for slab sample geometry to study anisotropic thermal transport properties of  $\mu\text{m}$ -thin crystalline films

*Rev. Sci. Instrum.* (April 2014)

Abrasive Wear Resistance of Tool Steels Evaluated by the Pin-on-Disc Testing

*AIP Conference Proceedings* (May 2011)



Optimize  
Your  
Research

New Vacuum Gauge Provides  
More Process Control  
and Operational Reliability



PFEIFFER  VACUUM

# Thermal conductivity versus depth profiling of inhomogeneous materials using the hot disc technique

A. Sizov,<sup>1</sup> D. Cederkrantz,<sup>1</sup> L. Salmi,<sup>2</sup> A. Rosén,<sup>3</sup> L. Jacobson,<sup>4</sup> S. E. Gustafsson,<sup>3</sup> and M. Gustavsson<sup>1,a)</sup>

<sup>1</sup>Hot Disk AB, Sven Hultins Gata 9A, SE-412 88 Gothenburg, Sweden

<sup>2</sup>Spinwest FoU AB, Lokattsbacken 54, SE-426 74 Gothenburg, Sweden and Närhälsan, Västra Götalandsregionen, Gothenburg, Sweden

<sup>3</sup>Department of Physics, University of Gothenburg, SE-412 96 Gothenburg, Sweden

<sup>4</sup>Chalmers Industriteknik, Sven Hultins Gata 9D, SE-412 88 Gothenburg, Sweden

(Received 10 March 2016; accepted 16 June 2016; published online 1 July 2016)

Transient measurements of thermal conductivity are performed with hot disc sensors on samples having a thermal conductivity variation adjacent to the sample surface. A modified computational approach is introduced, which provides a method of connecting the time-variable to a corresponding depth-position. This allows highly approximate—yet reproducible—estimations of the thermal conductivity vs. depth. Tests are made on samples incorporating different degrees of sharp structural defects at a certain depth position inside a sample. The proposed methodology opens up new possibilities to perform non-destructive testing; for instance, verifying thermal conductivity homogeneity in a sample, or estimating the thickness of a deviating zone near the sample surface (such as a skin tumor), or testing for presence of other defects. © 2016 Author(s). All article content, except where otherwise noted, is licensed under a Creative Commons Attribution (CC BY) license (<http://creativecommons.org/licenses/by/4.0/>). [<http://dx.doi.org/10.1063/1.4954972>]

## I. INTRODUCTION

### A. Homogeneous materials

When measuring the thermal conductivity and thermal diffusivity of a material with the hot disc technique,<sup>1–6</sup> a probe is typically placed between two sample pieces of the same material. Alternatively, a probe may be brought into contact with a single sample by clamping the probe to the sample by using a low-conducting material on the opposite side of the sensor. One may consider other means of applying a probe to a single sample, for instance using an adhesive, and then creating a vacuum or an environment with very low thermal conductivity outside the sample.<sup>7–9</sup> When performing an experiment according to the international standard ISO 22007-2,<sup>6</sup> it is understood that the material being analyzed is homogeneous.

In the basic methodology,<sup>1</sup> a single-step electrical heating current is applied to a hot disc probe, resulting in a well-defined heat input to the sample. Simultaneously, the temperature increase vs. time of the hot disc probe is recorded—typically a 2–5 °C temperature increase is reached. A theoretical model, involving a “shape function,”<sup>6</sup> is then fitted with the data points. In case the sample material is fully homogeneous, standard temperature deviations between measured points and the best-fit model can be as low as 50 μK, also for situations in which most data points (95%) are incorporated in the model fitting.<sup>5,6,10</sup> The numerical filtering-out of thermal contact effects between the probe and the sample, combined with an excellent fit of the experimental data to the physical model,

makes it possible to achieve a high-sensitivity analysis of thermal conductivity.

In transient measurements with the hot disc method, it has been shown that the thermal depth of probing, or “probing depth,” can be modeled as<sup>6</sup>

$$d_p = 2\sqrt{a \times t}. \quad (1)$$

Here  $a$  is the thermal diffusivity of the sample and  $t$  is the time measured from the start of the experiment. The numerical factor 2 is an empirical finding.<sup>6</sup> The probing depth makes it possible to visualize the geometrical zone in the sample—around the probe—where temperature increases in a way that has a measurable impact on the recorded temperature vs. time data.

### B. Inhomogeneous materials

#### 1. Geometry assumption

There are various approaches to testing an inhomogeneous material. For instance, an inhomogeneous geometrical configuration in the shape of a stack of thin layers is locally inhomogeneous when considering length scales on the order of the thickness of an individual layer. The same is true with a matrix material, incorporating a filler material. On a local scale, i.e., on the length scale of the geometrical irregularity, the material is obviously inhomogeneous. On a larger scale, however, a sample consisting of a matrix with a filler material can be assumed to exhibit approximately continuum behavior, with an averaged apparent bulk thermal conductivity and bulk thermal diffusivity. In addition, if the local irregularities are evenly distributed across the entire composite sample

<sup>a)</sup>Author to whom correspondence should be addressed. Electronic mail: [mattias.gustavsson@hotdiskinstruments.com](mailto:mattias.gustavsson@hotdiskinstruments.com).

structure, the apparent bulk properties behave approximately as a homogeneous material.

To achieve an experiment in which averaged—approximately homogeneous—material properties are estimated, a rule-of-thumb for a hot disc experiment is to ensure the selection of a hot disc sensor diameter much larger than the length scale of the local geometrical irregularity, and that the thermal depth of probing exceeds at least 10 such irregularities (e.g., a stack sample should consist of at least 10 layers on each side of the hot disc sensor when testing a stack setup, or, e.g., the thermal depth of probing should exceed 10 mean-free path distances between filler particles when testing a material composite based on a matrix with filler inclusions).<sup>5</sup>

There are different indicators of thermal conductivity inhomogeneity in a sample: for instance, different results of thermal conductivity, when positioning the sensor at different spatial positions across a sample surface, is a clear indicator of inhomogeneity.

In addition, tests may indicate the existence of a thermal conductivity gradient adjacent to a sample surface: for instance, if performing tests at the same surface position, using different sizes of hot disc sensors, using the original procedure,<sup>6</sup> one would obtain averaged results covering different probing depths. In case these averaged thermal conductivity results would prove to change with probing depth, this would also indicate inhomogeneity.

However, the following question is posed and analyzed in the present paper: Is it possible to attempt to estimate the thermal conductivity variation vs. depth by considering a single experiment, tested with a single sensor, at only one surface position?

## 2. Thermal conductivity variation versus thermal depth of probing

A first question concerns whether a physical model can be developed which directly computes the thermal conductivity variation vs. depth, by utilizing only temperature vs. time data as model input.

There is, to the authors' knowledge, no evidence of any inverse mathematical analysis capable of providing a unique solution for this problem. To illustrate the challenges such a general inverse problem poses, one may begin by considering the hypothetical situation of a perfectly controlled 1-dimensional heat-propagation setup applied to an inhomogeneous material. It can be shown that a hypothetical material

which is inhomogeneous in terms of thermal conductivity and thermal diffusivity vs. depth, but simultaneously homogeneous in terms of thermal effusivity ( $E = \lambda/\sqrt{a}$ , where  $\lambda$  is the thermal conductivity) vs. depth, will yield an identical temperature vs. time output signal at the sample surface, as compared to the situation when an experiment is performed on a fully homogeneous material with identical thermal effusivity.

Instead of directly attempting to mathematically invert the problem, another question is if it is possible—by some means of iteration or recursion formula—to attempt to approximately obtain thermal conductivity vs. depth information? Lacking a physical model developed specifically for inhomogeneous samples, is it possible to utilize existing models developed originally for homogeneous materials in an iteration scheme? If so, what assumptions need to be made? What accuracies and sensitivities are possible to achieve in a thermal conductivity vs. depth profiling algorithm? And finally, what specific experimental setup criteria are required to achieve a valid experiment? These questions are addressed in the following.

## II. THEORY

### A. Proposed iteration scheme

Considering Eq. (1), one may argue that a viable starting point would be an initial thermal conductivity value obtained at the most-shallow depth possible, utilizing the regular data-fitting procedure on data points corresponding to a minimum time window (with reasonable outcome, i.e., not too noisy results). By reducing the time window to a minimum, an estimation of “averaged” thermal conductivity properties within the depth zone  $[0, d_p(t_{\min})]$  would be obtained.

A means to minimize this initial time window would be to increase data sampling rate as much as possible and also assume an *a-priori*-known volumetric specific heat value of the sample. This insertion of the specific heat value in the data fitting procedure has the effect of stabilizing the estimation of the thermal conductivity—despite the fact that perhaps only a few data points (e.g., 10-20 data points) are used for the computation,<sup>11,12</sup> cf., e.g., Table I.

To estimate the thermal conductivity at deeper depths, one needs to perform computations over longer test times  $t_x$ .

The approach used in the present work involves performing a computation across a short time window, fixed in length, i.e., the same number of data points is utilized for each model fitting, but with an incrementally increasing starting time point of this time window. Hence, computations are made over

TABLE I. Estimations of thermal conductivity ( $\lambda$ ) in short time windows from a transient curve (for testing isotropic, homogeneous stainless steel), assuming a fixed specific heat capacity per unit volume ( $\rho c_p$ ). The short time windows utilize 21 data points only, from nominally 200 data points representing the total transient curve. The average thermal conductivity based on data points 14-200 is estimated at 13.551 W/mK (standard deviation 0.055%), while the average volumetric heat capacity is for points 14-200 estimated at 3.738 MJ/m<sup>3</sup> K (standard deviation 0.3%).

Data point window	10-30	30-50	50-70	70-90	90-110	110-130	130-150
$\rho c_p$ (MJ/(m <sup>3</sup> K))	3.738-fixed						
$\lambda$ (W/(mK))	13.589	13.516	13.628	13.666	13.555	13.553	13.615
Std. dev. (%)	0.18	0.75	1.29	0.96	0.88	0.76	0.75

the entire set of short time windows,  $[t_x, t_x + t_{min}]$ , where  $t_x$  starts from  $t_x = 0$  and ends at  $t_x = t_{max} - t_{min}$ , utilizing the homogeneous model, and assuming an *a-priori*-known volumetric specific heat value of the sample. This proposed procedure appears to provide highly reproducible thermal conductivity output, rendering thermal conductivity *vs.*  $t_x$  plots. (High reproducibility is also obtained for homogeneous samples, cf., e.g., in Table I.)

In Appendix A, a recursive scheme for estimating the thermal penetration depth is presented. This makes it possible to plot estimations of the thermal conductivity *vs.*  $d_p$ .

## B. Assumptions and consequences

For an experimental configuration where the sample is truly homogeneous, and the assumed *a priori* volumetric specific heat is reasonably estimated, the proposed iteration scheme will compute a thermal conductivity *vs.* depth output, which is accurate, stable, and reproducible. This holds true for situations when the sample geometry is perfectly 1-dimensional, as well as when the sample and sensor geometry assumes the original hot disc technique.<sup>1</sup> Table I illustrates the ability to extract accurate and stable thermal conductivity values computed in different short time windows within the entire  $T$ - $t$  curve, from a real experiment of stainless steel where heat flow occurs in a 3D manner.

However, considering Eq. (1), it should be noted that the numerical constant 2 is based on an empirical result. For instance, in 1-dimensional FEM simulations in Fig. 1, a significant decrease in thermal conductivity is computed at 1 mm depth, indicating that the constant 2 in Eq. (1) is fairly correct. The computations of depth position of cavities and copper slabs in experimental 3D tests in Figs. 2(a) and 3(a), respectively, appear correctly computed with Eq. (1). However, the thermal conductivity decrease in Fig. 2(b) and increase in Fig. 3(b), in 1-dimension FEM simulations, indicate that the constant 2 in Eq. (1) could have been selected with a slightly higher value.

For a homogeneous material, it should be noted that in case an offset specific heat value is deliberately selected, the iteration algorithm will result in a thermal conductivity *vs.*

depth, which will vary approximately according to a straight line with a non-zero slope.

For experimental situations, as well as in FEM simulations, as illustrated in Figs. 2 and 3, where an initial zone is fully homogeneous, followed by a sudden shift of thermal conductivity value at a certain depth, it is clear that the proposed iteration scheme does not capture the true thermal conductivity behavior. Arguably, the thermal conductivity value computed for time window  $[t_x, t_x + t_{min}]$  is heavily influenced by the thermal conductivity at shallower depths. This observation has direct effect on the sensitivity and accuracy of the proposed method. Arguably, the sensitivity is significantly reduced at greater probing depths. This can be observed in Fig. 1(b), where the shift from 2 W/mK to 1.5 W/mK at 1 mm depth results in a quick decrease in computed thermal conductivity *vs.* depth in the depth zone from 1 mm to 2 mm depth. However, a new shift at 2 mm depth does not result in the thermal conductivity estimation to equally swiftly return to the 2 W/mK value at depths deeper than 2 mm.

## III. EXPERIMENTAL CRITERIA

A first key to devising a usable and valuable experiment is to have some idea of the nature of the inhomogeneity of interest to be tested. Is the sample inhomogeneous at all? Do we expect some spatial gradient? Or are we looking at some local defect, at the surface, or looking for some defect, at sub-surface depths? What is the length scale of inhomogeneity we wish to analyze? Or do we wish to confirm sample homogeneity, cf., e.g., Appendix B? Do we wish to monitor thermal conductivity *vs.* depth, which may change with time scales much longer than an individual hot disc experiment (for instance, monitoring thermal conductivity *vs.* depth on human skin, when applying some skin lotion or skin cream)?

A second key is to consider a suitable selection of sensor size. The sensor size selection connects with the length scale of the inhomogeneity of interest to analyze. For instance, in case an inhomogeneity variation in the direction from the sensor plane into the sample material is to be analyzed, it can be noted that for situations in which the total test time  $t_{max}$  is much shorter than the average “characteristic” time

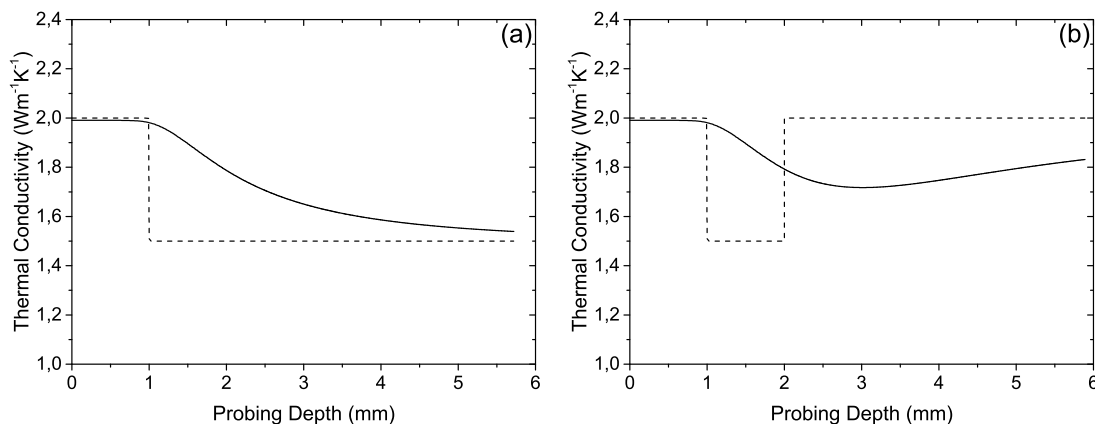


FIG. 1. Estimation of thermal conductivity *vs.* depth (solid line), for a numerically simulated situation in which the true thermal conductivity is varying (dotted line): (a) in a step-wise manner with depth, (b) in two steps with depth.

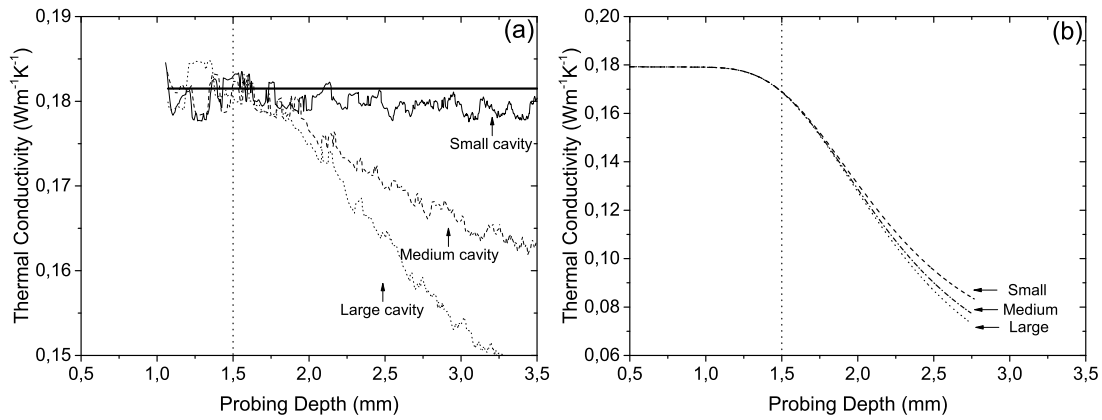


FIG. 2. Thermal conductivity versus penetration depth of a rubber composite (a) with an internal defect (insulating air cavity) placed at a distance of 1.5 mm from the sensor in the normal direction (volumes of small, medium, and large air cavities are 4.1, 31.8, and 63.6  $\text{mm}^3$ , respectively). Experiments allow a 3D heat flow around the sensor and cavities. (b) Numerical simulations results in 1D with different-sized air gap (small, medium, and large), placed at a distance of 1.5 mm from the sensor. (Regarding quantitative differences in 3D experiments and 1D simulations, cf. discussion in Section IV.)

of the sensor ( $\theta = r^2/a_{av,in-plane}$ , where  $r$  is the radius of the hot disc sensor), e.g.  $t_{max} < 0.1\theta$ , the 3D shape function is almost identical to the shape function of the corresponding 1D experiment. That is, for such short-time tests, the sensor mainly detects the thermal conductivity variation in the normal direction (sideways heat flow—in the sensor plane—always exists, but only has a significant influence on the outcome on test times greater than  $t_x > 0.1\theta$ ). This relation also holds true for anisotropic samples. It can, in this context, be observed that for a standard, homogeneous 3D hot disc test, test times are generally recommended to be performed in such a way that the total test time fulfills the criterion  $0.33 < t_{max}/\theta < 1$ . It can also be noted that for a near-isotropic sample,  $t_{max} < 0.1\theta$  corresponds approximately to  $d_{p,max} < 0.3 \times \text{sensor diameter}$ .

A number of “scouting tests” are often required. Such scouting tests are, for instance, valuable in order to obtain initial rough data on averaged thermal conductivity and averaged thermal diffusivity, which are useful in the selection of operating parameters such as heating power and test time duration.

For a near-isotropic sample, the selected volumetric specific heat value used in the iterations should be selected near the real volumetric specific heat value. This also applies for

tests performed fulfilling the relation  $t_{max} < 0.1\theta$ , in order for the thermal conductivity estimations to represent the through-plane thermal conductivity of the tested material. As regards the real volumetric specific heat value, one should note that for dense, inert materials at room temperature conditions, the volumetric specific heat value is typically within the range 1-4  $\text{MJ/m}^3 \text{ K}$ .<sup>13</sup>

It should also be mentioned that the sensor size might need to be selected with respect to the type of defect one would be looking for. For instance, the authors are not presently able to provide any general information on which sensor would be most suitable for the detection of a sharp, sub-surface defect, such as a cavity, or larger crack. That is, which sensor size is best suited to detect a hypothetical geometrical deviation? For instance, Figs. 2 and 3 illustrate some laboratory examples in which different deviations are built into a sample. An alternative to perform laboratory experiments would be to perform numerical FEM simulations, to gain additional insight on experimental sensitivity.

Other experimental criteria to consider are imperfect thermal contact at the sample surface, and also the effect of the pertaining sensor insulation material on the initial data points. By analysis of experimental data, one often finds

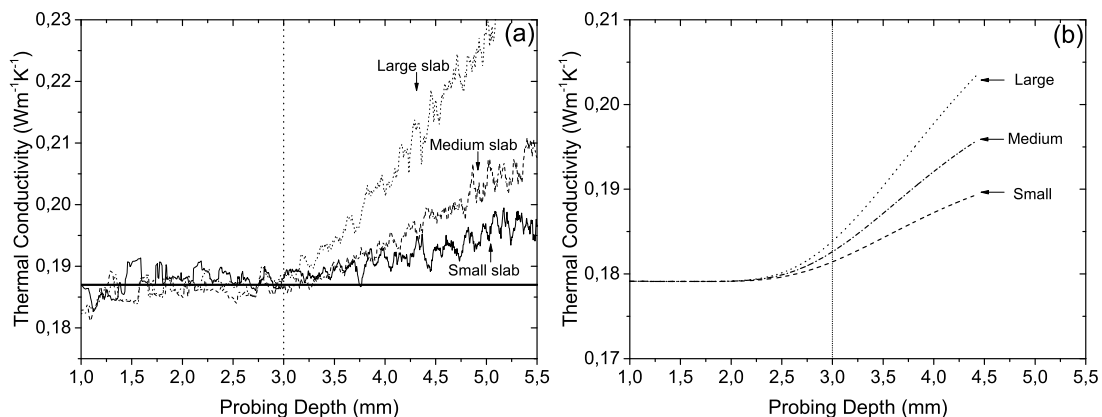


FIG. 3. Thermal conductivity vs. penetration depth of a rubber composite (a) with an internal defect (“heat sink”) placed at a distance of 3 mm from the sensor in the normal direction (volumes of small, medium, and large copper slabs are 13.3, 26.6, and 53.2  $\text{mm}^3$ , respectively). Experiments allow a 3D heat flow around the sensor and the copper slabs. (b) Numerical simulation results in 1D with differently sized high-conducting material (small, medium, and large), placed at a distance of 3 mm from the sensor. (Regarding quantitative differences in 3D experiments and 1D simulations, cf. discussion in Section IV.)



situations in which initial data points deviate strongly due to imperfect thermal contact between the sample surface and sensor. For instance, for a hard sample with a rough surface, the applied time-constant heat input at the sensor probe—for a single-sided experimental setup—may not provide a time-constant heat input into the sample of interest.<sup>14</sup> Calculated graphs of thermal conductivity vs. depth may indicate sharp inhomogeneity gradients at the near surface zone, which are unrealistic. Hence, one should expect a certain zone, maybe comprising the first 2% data points, as useless data. For a collection-rate of 100 data points per second, the first 2% data points (of 2000 data points) represent a removal of initial time points of 0.4 s (40 initial data points). This corresponds to cutting out the initial depth zone from surface to the depth  $2\sqrt{a_{av} \times 0.4 \text{ s}}$  from the inhomogeneity analysis. To illustrate, when testing for instance a stainless steel sample at room temperature conditions, the present approach only allows analysis at probing depths deeper than 2.5 mm. For tests on human skin, the present approach only allows analysis at probing depths deeper than 0.4 mm, cf., [Appendix C](#).

#### IV. SUMMARY AND CONCLUSIONS

The experimental methodology of the presently proposed technique is similar to the original hot disc method. The experimental technique is based on applying a single-step constant heat flow input at a sample surface in combination with simultaneous recording of the temperature increase with time (at the same position as where heat flow input is applied). The same experimental apparatus and sensors can be used in the proposed technique. Also, the original physical model developed for homogeneous samples is retained—however, calculations are made using an iteration scheme involving small time windows and a recursive formula to connect time stamps with depth position data.

The outcome of the calculation scheme described above is a highly approximate, smoothened-out picture of the thermal conductivity variation with probing depth. A direct consequence of this is that the proposed method should not be understood as an accurate thermal conductivity depth-profiling tool. Rather, it should be viewed as a non-destructive evaluation tool, to assist in making judgements on possible structural gradients (which might influence the local thermal conductivity): One advantage is the high degree of reproducibility of this technique (cf. [Appendix B](#)). In case one would perform tests on dense samples, such as biological materials, which can be assumed not to incorporate solid-solid thermal contact resistance interfaces, voids etc., and where the average volumetric specific heat is fairly uniform throughout the sample,<sup>13</sup> it is believed possible to make estimations of thicknesses of a deviating structure, as compared to a reference structure (cf. [Appendix C](#)).

The presence of sharp inhomogeneities, such as thin contact resistances within the sample or high-conducting heat sinks, may admittedly present challenges in interpretations of results. It is therefore advised that model tests be performed in laboratory conditions or by FEM simulations. The authors believe that FEM simulations in 3D which closely match an

experimental situation, may indicate better the ability and sensitivity of this technique. (The 1D FEM modelling made in the present work only serves to demonstrate the accuracy of the numerical factor 2 in Eq. (1), cf. Fig. 1(a), and also to qualitatively demonstrate different outcomes when selecting different-sized air cavities and different-sized conducting slab sheets, cf. Figs. 2(b) and 3(b).) In particular, when a tested sample contains cavities with a void or with a medium of significantly different volumetric specific heat—which apparently offsets the model assumption on fixed volumetric specific heat throughout the sample (cf. [Appendix A](#))—it is believed that FEM simulations may prove useful in assessing the influence on thermal conductivity output.

#### ACKNOWLEDGMENTS

The present study has been financially supported by VINNOVA.

#### APPENDIX A: CALCULATION SCHEME

The following scheme is implemented: A moving time window based on data points  $[i, i + N]$  is analyzed, corresponding to an analysis within the time window  $(t_1, t_2) = [t(i), t(i + N)]$ . Assume  $N = 30$  points.

Start with time window  $[t(0), t(N)]$ . Compute the thermal conductivity  $\lambda(N)$  for this time window. In this initial step the average thermal conductivity  $\lambda_{av}(N) = \lambda(N)$ . From known specific heat value, compute average thermal diffusivity  $a_{av}(N) = \lambda_{av}(N) / \rho c_p$ . The depth position,  $d_p[t(N)]$ , is computed from Eq. (1) using  $a = a_{av}(N)$ . For the following iterations,  $x(N)$  is computed by  $x(N) = d_p[t(N)]$ , and  $R(N) = [x(N) - x(0)] / \lambda_{av}(N)$ , where  $x(0) = 0$ .

In next step, computation is made from time window  $[t(1), t(N + 1)]$ , by which  $\lambda(N + 1)$  is computed.

The following iteration is required to be solved to determine the depth position  $x(N + 1)$ :

$$R(N + 1)^* = R(N) + [x(N + 1)^* - x(N)] / \lambda(N + 1), \quad (\text{A1})$$

$$\lambda_{av}(N + 1)^* = [x(N + 1)^* - x(0)] / R(N + 1)^*, \quad (\text{A2})$$

$$a_{av}(N + 1)^* = \lambda_{av}(N + 1)^* / \rho c_p, \quad (\text{A3})$$

$$x(N + 1)^* = d_p[t(N + 1)]^* = 2\sqrt{a_{av}(N + 1)^* \times t(N + 1)}. \quad (\text{A4})$$

Equations (A1)–(A4) are repeated until stable values appear for the iterated parameters (marked with \*).

Repeat the above step, for time windows  $[t(2), t(N + 2)]$ ,  $[t(3), t(N + 3)]$ , ...,  $[t(2000 - N), t(2000)]$ .

Hence, it is possible to plot  $\{\lambda(N), \lambda(N + 1), \lambda(N + 2), \dots, \lambda(2000)\}$  versus  $\{x(N), x(N + 1), x(N + 2), \dots, x(2000)\}$ .

#### APPENDIX B: MEDICAL TABLETS

Thermal conductivity vs. probing depth for vitamin C tablets from three different producers are presented in Fig. 4(a). Each tablet pair was tested twice, in fully dry

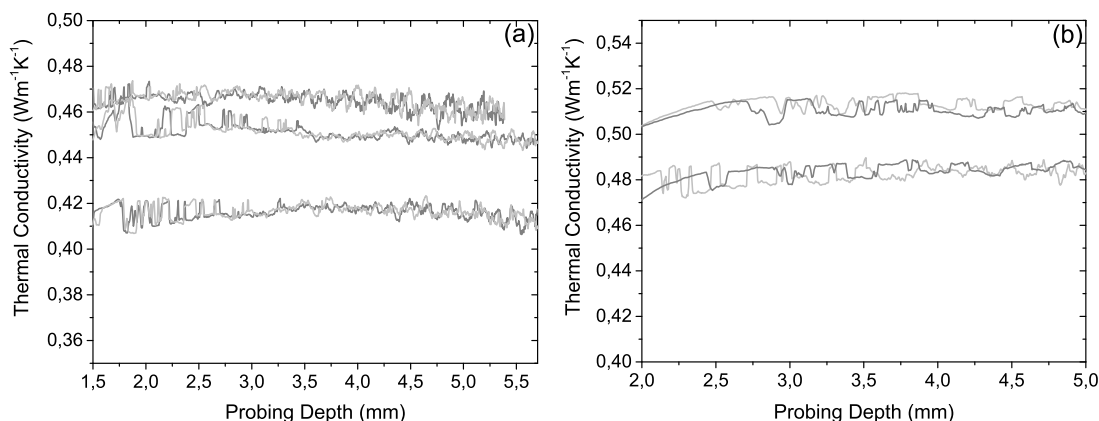


FIG. 4. (a) Thermal conductivity vs. probing depth for vitamin C tablets from three different producers. (b) Thermal conductivities vs. probing depth of aspirin tablets from different batches, but same producer.

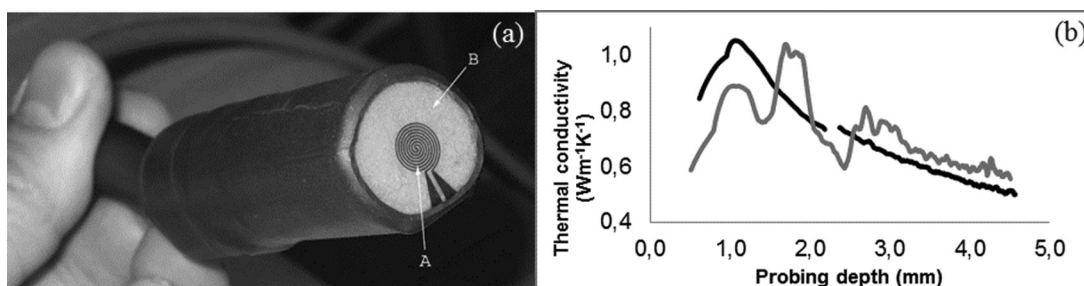


FIG. 5. (a) Structural probe with a 7 mm diameter hot disc sensor (A is an active part of the sensor; B is an insulating material on the backside of the sensor). (b) Thermal conductivity depth profile a few mm beneath the surface. Measurement time is around 20 s. Measurements are non-invasive, involve no radiation, and no electrical contact with the sample. Only a slight temperature increase of 3–4 °C is required. (In the black curve, a slight movement of the operator occurred during the experiment, resulting in a slight temperature offset. This offset in turn resulted in a small region of deviating points, which were removed in the above graph.)

atmospheric conditions and at room temperature. These results imply that the tablets are fairly homogeneous. Also, repeated tests imply that the results regarding thermal conductivity vs. depth are reproducible. Probably due to differences in manufacturing of the tablets at the different producers, the absolute values of thermal conductivity appear different.

In Fig. 4(b) the thermal conductivities vs. probing depth of aspirin tablets are depicted. Tablet pairs from the same producer are taken, where, however, different batches are compared. Tests are performed in fully dry atmospheric conditions, at room temperature. Some 6%–7% differences in absolute values can be observed, probably due to differences in batch. For these aspirin tablets, the thermal conductivity vs. depth appears to display a fairly homogeneous sample structure with depth.

## APPENDIX C: SKIN CANCER

Tests are conducted with a single-sided probe, resembling a stethoscope-type probe, cf. Fig. 5(a). In Fig. 5(b), a reference test on human skin (next to the tumor) is depicted by the black curve. The test on the tumor is then depicted by the grey curve. Comparing grey and black curves, the structure of the tumor appears deviating from the comparison skin, down to a depth of approx. 2.7 mm from the surface. At deeper depths, i.e. deeper than approx. 2.7 mm (in the subcutaneous skin zone), the two

curves appear similar in shape. The interpretation made here is that the depth zone deeper than 2.7 mm is outside the zone of the tumor. The latter has been verified in microscopy tests of the relevant skin sample.

<sup>1</sup>S. E. Gustafsson, *Rev. Sci. Instrum.* **62**, 797 (1991).

<sup>2</sup>S. E. Gustafsson, B. Suleiman, N. S. Saxena, and I. U. Haq, *High Temp.–High Pressures* **23**, 289 (1991).

<sup>3</sup>M. Gustavsson, E. Karawacki, and S. E. Gustafsson, *Rev. Sci. Instrum.* **65**, 3856 (1994).

<sup>4</sup>T. Log and S. E. Gustafsson, *Fire Mater.* **19**, 43 (1995).

<sup>5</sup>M. Gustavsson and S. E. Gustafsson, in *Proceedings of the 26th International Thermal Conductivity Conference, Massachusetts, Cambridge, 6–8 August 2001*, edited by R. Dinwiddie (Oak Ridge National Laboratory, Oak Ridge, Tennessee, 2004), pp. 367–377.

<sup>6</sup>ISO, 22007–2, “Plastics—Determination of thermal conductivity and thermal diffusivity—Part 2: Transient plane heat source (hot disc) method.”

<sup>7</sup>S. E. Gustafsson, E. Karawacki, and M. N. Khan, *J. Phys. D: Appl. Phys.* **12**, 1411 (1979).

<sup>8</sup>S. E. Gustafsson, E. Karawacki, and M. N. Khan, *J. Appl. Phys.* **52**, 2596 (1981).

<sup>9</sup>S. E. Gustafsson, M. A. Chohan, K. Ahmed, and A. Maqsood, *J. Appl. Phys.* **55**, 3348 (1984).

<sup>10</sup>D. Lundström, B. Karlsson, and M. Gustavsson, *Z. Metallkd.* **92**, 1203 (2001).

<sup>11</sup>B. M. Suleiman, M. Gustavsson, E. Karawacki, and A. Lundén, *J. Phys. D: Appl. Phys.* **30**, 2553 (1997).

<sup>12</sup>H. Nagai, Y. Nakata, T. Tsurue, H. Minagawa, K. Kamada, S. E. Gustafsson, and T. Okutani, *Jpn. J. Appl. Phys., Part 1* **39**, 1405 (2000).

<sup>13</sup>M. Gustavsson and S. E. Gustafsson, *Thermochim. Acta* **442**, 1 (2006).

<sup>14</sup>M. Gustavsson, H. Nagai, and T. Okutani, *Solid State Phenom.* **124–126**, 1641 (2007).